Biointerface Research in Applied Chemistry
Open-Access Journal (ISSN: 2069-5837)

Article
Volume 16, Issue 3, 2026, 87
https://doi.org/10.33263/BRIAC163.087

M-Polynomial Driven QSPR Modeling for Mechanical Characteristics of Single-Layer Borophene Nanosheets

Deekshitha K V [1,*], Shrikanth A S [2], Sumithra, Kavya B R

[1] Department of Mathematics, Malnad College of Engineering, affiliated to Visvesvaraya Technological University,, Hassan – 573202, India; kvdeekshitha.77@gmail.com;
[2] Department of Mathematics, Adichunchanagiri Institute of Technology, affiliated to Visvesvaraya Technological University,, Chikkamagaluru - 577102, India; shrikanthas@gmail.com;
[3] Department of Mathematics, NIE Institute of Technology, affiliated to Visvesvaraya Technological University,, Mysuru - 570008, India; sumithra@nie.ac.in;
[4] Department of Civil Engineering, Adichunchanagiri Institute of Technology, affiliated to Visvesvaraya Technological University, Chikkamagaluru - 577102, India; br.kavya6@gmail.com;
* Correspondence: kvdeekshitha.77@gmail.com;

Received: 9.12.2025; Accepted: 6.05.2026; Published: 15.06.2026

Abstract: Borophene, with its outstanding mechanical and electronic properties, is a promising material for advanced technological applications. This work applies concepts from chemical graph theory to examine five single-layered borophene nanosheets by deriving their M-polynomials and computing various Degree-based Topological Indices (DBTI). These indices are correlated with key mechanical properties - Young's modulus, Poisson's ratio, strain at ultimate tensile strength, and ultimate tensile strength. Further linear, quadratic, cubic, exponential, and logarithmic regression models were examined, and based on the coefficient of determination (R^2) value, the most appropriate model was identified. Thus, the study demonstrates that M-polynomial–based descriptors offer an efficient and reliable framework for predicting the mechanical behavior of borophene nanosheets.

Keywords: borophene; topological indices; M-polynomial; mechanical properties; regression models.

1. Introduction

Chemical graph theory has its historical roots in concepts like chemical connectivity, graph matrices, symmetry, and transformations. These principles play a key role in establishing its framework for modeling chemical structures through graphs [1]. In this scenario, topological indices (TIs) are crucial, as they encode molecules as graphs with vertices corresponding to atoms and edges corresponding to chemical bonds [2]. According to IUPAC, a topological index is a numerical value used to evaluate a chemical structure and correlate it with many physical properties, reactivity, and biological activity [3]. These indices, which form the core of Quantitative Structure-Property Relationships (QSPR) and Quantitative Structure-Activity Relationships (QSAR), are critical for predicting structural and functional properties such as stability, boiling point, and toxicity [4–7].

In the field of mathematical chemistry, the calculation of structural descriptors has relied on direct computation from their definitions, a process that is typically laborious. Building on these advancements, Deutsch and Klavžar [8] introduced the concept of the M-polynomial in 2014. M-polynomial provides a general polynomial-computation approach that enables efficient calculation of various degree-based structural descriptors, facilitating the process and expanding its applicability for capturing structural and chemical properties.

Boron is found in the periodic table between metals and non-metals. Due to its exceptional chemical and physical properties, it can create low-dimensional structures like borophene. The unfolding of borophene significantly led the progress of the field of two-dimensional (2D) nanomaterials. The remarkable mechanical strength, electrical conductivity, chemical stability, and thermal resilience of borophene have sparked a great deal of study curiosity [9]. Owing to its unique properties, borophene holds great potential for use in a variety of industries, such as biomedicine [10], energy storage [11], and memory devices [12].

Munir *et al*. [13] reported the M-polynomials of single-walled titania (SW TiO2) nanotubes, a nanostructure of great interest due to its numerous applications in the manufacture of corrosion-resistant, gas-sensing, and catalytic materials. Munir *et al*. [14] studied M-polynomials of boron triangular nanotubes and recovered numerous significant topological degree-based indices of these nanotubes and demonstrated how each topological index depended on the structural characteristics. Li *et al*. [15] obtained closed forms of certain degree-based topological indices of linear chains of graphs of benzene, naphthalene, and anthracene, as well as M-polynomials bringing in the correlation between these indices on the fundamental building blocks of these three chains.

The work of Afzal *et al*. [16] demonstrated that the molecular structure of boron α-nanotube contains the topological indices that were used to decipher the information. Liu *et al* [17] provided the extension of m-polynomial and degree-based topological indices for two nanotubes, HC_5C_7(A) and VC_5C_7(B). With advances in the study of coronoid polycyclic aromatic hydrocarbons, driven by their evolving applications in nanotechnology, research in this field has become much more prominent. The computation of the various degree-based topological indices for coronoid structures with cavities that vary depending on their topology using the M-polynomial was made by Julietraja and Venugopal [18]. Khan *et al*. [19] computed the first and second temperature indices, the sum connectivity temperature index, the hyper temperature indices, the product connectivity temperature index, the reciprocal product connectivity temperature index, and the F temperature index of a molecular graph SiO4 embedded in a chain. The molecular structure of SiO4 provides strong motivation for the exploration of all the interconnected networks.

The M-polynomial technique is utilized to establish the degree-based descriptors of the β_{12}-Borophene nanosheet by Ismail *et al*. [20]. Further, based on the identified analytic expressions, a numerical and graphical comparison is also presented. The study by Nagesh [21] employed QSPR models incorporating temperature-based topological indices, such as the sum connectivity, product connectivity, F-temperature, and symmetric division temperature indices, to predict thermodynamic properties of monocarboxylic acids. These analyses provide fundamental connections between thermodynamic parameters and topological indices by using linear, quadratic, and cubic curvilinear regression models. Khan *et al*. [22] calculated temperature indices for borophene nanosheets and used them in a QSPR analysis of the properties of two borophene nanosheets, including Poisson's ratio, Young's modulus, and Shear modulus.

The M-polynomials of fractal benzene structures, Pythagoras trees, and benzene dendrimers and their degree-based topological indices were obtained by Sarhan *et al*. [23]. This work analyzed the structural patterns and trends in iterative molecular graphs. Wasim Sajjad *et* *al*. [24] examined carbon nanotubes as chemical graphs and calculated topological invariants based on eccentricity, such as eccentric-connectivity, total-eccentricity, and Zagreb indices, to reveal their structural and physicochemical properties. The correlation between degree-based topological indices and entropy measures was studied using M-polynomials for porous graphitic frameworks, providing a glimpse into their structural properties [25]. M-polynomials were calculated for carbazole dendrimers [26] to derive degree-based topological indices, such as the Hyper Zagreb, Redefined Zagreb, and Reciprocal Randić indices, as proposed by Venkatesan et al., thereby providing a framework for QSPR analysis of dendritic molecular structures. An explicit expression of the M-polynomial was derived by Mehiri for generalized Hanoi graphs H_{pn} [27], allowing exact computation of degree-based topological indices and providing complete structural characterization.

Recent experimental breakthroughs in the synthesis of various borophene nanosheets have revealed a number of novel structures with promising technological applications, underscoring the importance of understanding their mechanical properties. As a boron counterpart of graphene, borophene has been shown to have several structural polymorphs, all of which display metallic properties. While a number of experimental and theoretical studies have investigated the structural, electronic, and mechanical properties of borophene, there is a lack of comprehensive quantitative structure-property relationships (QSPRs) that correlate mechanical properties with graph-theoretic molecular descriptors. Specifically, the application of degree-based topological indices within the M-polynomial framework to describe and compare the mechanical properties of different polymorphs of borophene [28] has not been sufficiently investigated, underscoring the significance of the current study.

The dataset considered in this study is necessarily small, as only a few polymorphs of borophene nanosheets have been discovered so far. This is because the field of borophene is still in its nascent stage, and experimental work on its synthesis is in its infancy.

2. Materials and Methods

In this article, all connectivity graphs are finite, connected, loopless, and have no multiple edges. The Graph $G(V, E)$ has the vertex set V and edge set E. The degree of the vertex $a \in V(G)$ is denoted by d_a is the total number of edges incident on the vertex a [29,30]. Let G be a graph and $m_{kl}(G), k,\ l \geq 1$ be the number of edges $ab \in E(G)$ such that $(d_a, d_b) = (k, l)$, the M –polynomial [8] is given by:

$$M(G; x, y) = \sum_{k \leq l} m_{kl}(G) x^k y^l \quad (1)$$

The computation of the degree-based topological indices using M-polynomial requires the following operators(a):

$$D_x(f(x, y)) = x\ \frac{\partial(f(x,y))}{\partial x} \quad (2)$$

$$D_y(f(x, y)) = y\ \frac{\partial(f(x,y))}{\partial y} \quad (3)$$

$$S_x(f(x, y)) = \int_0^x \frac{(f(x,y))|_{x=t}}{t} dt \quad (4)$$

$$S_y(f(x, y)) = \int_0^y \frac{(f(x,y))|_{y=t}}{t} dt \quad (5)$$

$$J(f(x, y)) = f(x, x) \quad (6)$$

$$Q_a(f(x, y)) = x^\alpha f(x, y);\ \ \alpha \neq 0 \quad (7)$$

$$L_x(f(x, y)) = f(x^2, y) \quad (8)$$

$$L_y(f(x, y)) = f(x, y^2) \quad (9)$$

A few important Degree-based Topological indices and their formulas for derivation from M-polynomial are given in Table 1.

Table 1. The M-polynomial formulas are used to derive the degree-based topological indices.

Degree-based TI	Notation	$f(x,y)$	$M(G:x,y)$ based derivation
First Zagreb [31]	$M_1(G)$	$x+y$	$(D_x+D_y)(M(G:x,y))\vert_{x=y=1}$
Second Zagreb [31]	$M_2(G)$	xy	$(D_xD_y)(M(G:x,y))\vert_{x=y=1}$
Second Modified Zagreb [32]	$M_2{}^m(G)$	$\frac{1}{xy}$	$(S_xS_y)(M(G:x,y))\vert_{x=y=1}$
Third Zagreb [33]	$M_3(G)$	$\lvert x-y\rvert$	$\lvert D_x-D_y\rvert(M(G:x,y))\vert_{x=y=1}$
Randic [4]	$R(G)$	$\frac{1}{\sqrt{xy}}$	$\left(D_x^{\frac{-1}{2}}D_y^{\frac{-1}{2}}\right)(M(G:x,y))\vert_{x=y=1}$
Nano Zagreb [34]	$N_z(G)$	$\lvert x^2-y^2\rvert$	$\lvert D_x{}^2-D_y{}^2\rvert(M(G:x,y))\vert_{x=y=1}$
Sum Nano Zagreb [35]	$\chi_{\frac{1}{2}}N_z(G)$	$\sqrt{\lvert x^2-y^2\rvert}$	$\sqrt{\lvert D_x{}^2-D_y{}^2\rvert}(M(G:x,y))\vert_{x=y=1}$
First Hyper Zagreb [36]	$HM_1(G)$	$(x+y)^2$	$(D_x+D_y)^2(M(G:x,y))\vert_{x=y=1}$
Sigma [37]	$\sigma(G)$	$(x-y)^2$	$(D_x-D_y)^2(M(G:x,y))\vert_{x=y=1}$
Symmetric Division [37]	$SDD(G)$	$\frac{x^2+y^2}{xy}$	$(D_xS_y+D_yS_x)(M(G:x,y))\vert_{x=y=1}$
Atom Bond Connectivity [38]	$ABC(G)$	$\sqrt{\frac{x+y-2}{xy}}$	$\left(\left(D_x^{\frac{-1}{2}}D_y^{\frac{-1}{2}}\right)*\left(D_x^{\frac{1}{2}}Q_{-2}J\right)\right)(M(G:x,y))\vert_{x=y=1}$
Geometric Arithmetic [39]	$GA(G)$	$\frac{2\sqrt{xy}}{x+y}$	$\left(2\left(D_x^{\frac{1}{2}}D_y^{\frac{1}{2}}\right)*(S_xJ)\right)(M(G:x,y))\vert_{x=y=1}$
Harmonic[40,41]	$H(G)$	$\frac{2}{x+y}$	$(2S_xJ)(M(G:x,y))\vert_{x=y=1}$
Sum Connectivity [42]	$SC(G)$	$\frac{1}{\sqrt{x+y}}$	$\left(S_x^{\frac{1}{2}}J\right)(M(G:x,y))\vert_{x=y=1}$
First k-Banhatti [43]	$B_1(G)$	$x+y+2(x+y-2)$	$((D_x+D_y)+2D_xQ_{-2}J))(M(G:x,y))\vert_{x=y=1}$
Second k-Banhatti [43]	$B_2(G)$	$(x+y-2)(x+y)$	$(D_xQ_{-2}J(D_x+D_y))(M(G:x,y))\vert_{x=y=1}$
Modified First k-Banhatti [44]	$m_{B_1}(G)$	$\frac{1}{x^2+y-2}+\frac{1}{x+y^2-2}$	$\left(S_xQ_{-2}J(L_x+L_y)\right)(M(G:x,y))\vert_{x=y=1}$
Modified Second k-Banhatti [44]	$m_{B_2}(G)$	$\left(\frac{1}{x}+\frac{1}{y}\right)\left(\frac{1}{x+y-2}\right)$	$\left(S_xQ_{-2}J(S_x+S_y)\right)(M(G:x,y))\vert_{x=y=1}$
Harmonic k-Banhatti [43]	$HB(G)$	$2\left(\frac{1}{x^2+y-2}+\frac{1}{x+y^2-2}\right)$	$\left(2S_xQ_{-2}J(L_x+L_y)\right)(M(G:x,y))\vert_{x=y=1}$

3. Borophene Structure Analysis

The five borophene sheets, namely S_1, S_2, S_3, S_4, S_5 as mentioned in [28], is considered directly where r is the number of rows and c is the number of columns. The connectivity graph of all five structures is depicted, taking $r = 4$ and $c = 4$ as it gives a complete picture of all possible vertex and edge set.

3.1. S_1 Borophene structure.

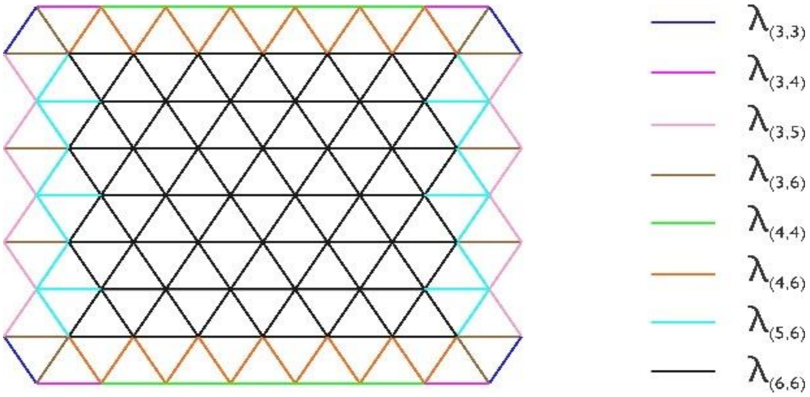

Figure 1. Edge partition of S_1 borophene structure.

Theorem 1: Let $G = S_1(r,c)$ such that $r,c \geq 1$ be the connectivity graph of the S_1-borophene nanosheet, as shown in the figure, then the M-polynomial is defined to be:

$$M(G;x,y) = 4x^3y^3 + 4x^3y^4 + (4r-4)x^3y^5 + (2r+4)x^3y^6 + (4c-6)x^4y^4 + (8c-8)x^4y^6 + (6r-6)x^5y^6 + (12cr-13r-10c+11)x^6y^6 \quad (10)$$

Proof:

Consider the connectivity graph $G = S_1(r,c)$; $r,c \geq 1$ with $|V(G)| = 4cr + r + 2c$ and $|E(G)| = 12cr + 2c - r - 1$. The partition of the edge set based on the vertex degree is given by $\lambda_{(k,l)} = \{(a,b) \epsilon E(G): d_a = k, d_b = l\}$. The connectivity graph of the S_1-borophene nanosheet is illustrated in Figure 1 and the corresponding M-polynomial representation is shown in Figure 2. It is observed that:

Edge partition	$\lambda_{(3,3)}$	$\lambda_{(3,4)}$	$\lambda_{(3,5)}$	$\lambda_{(3,6)}$	$\lambda_{(4,4)}$	$\lambda_{(4,6)}$	$\lambda_{(5,6)}$	$\lambda_{(6,6)}$
Cardinality	4	4	4r-4	2r+4	4c-6	8c-8	6r-6	12cr-13r-10c+11

By the definition of the M-polynomial, we get:

$$M(G;x,y) = \sum_{3\leq 3} m_{33}x^3y^3 + \sum_{3\leq 4} m_{34}x^3y^4 + \sum_{3\leq 5} m_{35}x^3y^5 + \sum_{3\leq 6} m_{36}x^3y^6 + \sum_{4\leq 4} m_{44}x^4y^4 + \sum_{4\leq 6} m_{46}x^4y^6 + \sum_{5\leq 6} m_{56}x^5y^6 + \sum_{6\leq 6} m_{66}x^6y^6 \quad (11)$$

$$= |\lambda_{(3,3)}|x^3y^3 + |\lambda_{(3,4)}|x^3y^4 + |\lambda_{(3,5)}|x^3y^5 + |\lambda_{(3,6)}|x^3y^6 + |\lambda_{(4,4)}|x^4y^4 + |\lambda_{(4,6)}|x^4y^6 + |\lambda_{(5,6)}|x^5y^6 + |\lambda_{(6,6)}|x^6y^6$$

$$= 4x^3y^3 + 4x^3y^4 + (4r-4)x^3y^5 + (2r+4)x^3y^6 + (4c-6)x^4y^4 + (8c-8)x^4y^6 + (6r-6)x^5y^6 + (12cr-13r-10c+11)x^6y^6$$

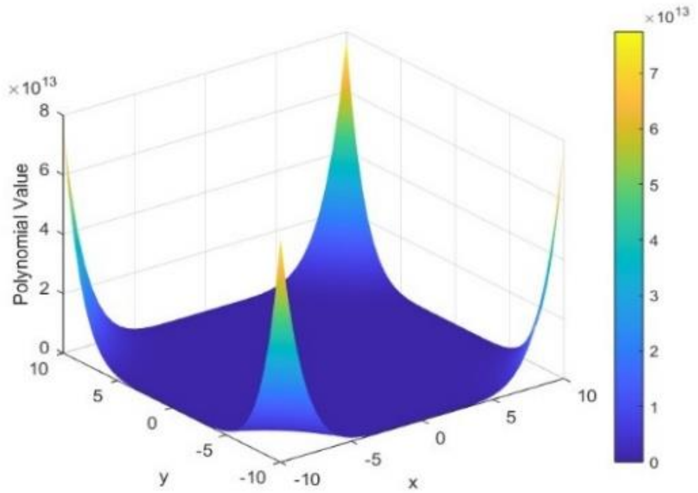

Figure 2. Graphical Representation of the M-polynomial for S_1 borophene structure.

Theorem 2: For $G = S_1(r,c)$ such that $r,c \geq 1$,

$$M_1(G) = 144cr - 40r - 80c - 6$$

$$M_2(G) = 432cr - 192r - 104c + 24$$

$$M_2{}^m(G) = \frac{11c}{36} + \frac{13r}{60} + \frac{cr}{3} + \frac{47}{360}$$

$$M_3(G) = 16c + 20r - 14$$

$$R(G) = 2cr - \frac{13r}{6} - \frac{2c}{3} + \frac{\sqrt{6}(8c-8)}{12} + \frac{\sqrt{2}(2r+4)}{6} + \frac{\sqrt{15}(4r-4)}{15} + \frac{\sqrt{30}(6r-6)}{30} + \frac{2382432804997525}{844424930131968}$$

$$N_z(G) = 160c + 184r - 154$$

$$\chi_{\frac{1}{2}}N_z(G) = 16r + 4\sqrt{7} + 2\sqrt{5}(8c-8) + 3\sqrt{3}(2r+4) + \sqrt{11}(6r-6) - 16$$

$$HM_1(G) = 1728cr - 728r - 384c + 82$$

$$\sigma(G) = 32c + 40r - 14$$

$$SDD(G) = \frac{16c}{3} + \frac{4r}{15} + 24cr - \frac{34}{15}$$

$$ABC(G) = \frac{8\sqrt{3}c}{3} + \sqrt{6}c - \frac{5\sqrt{10}c}{3} - \frac{41\sqrt{10}r}{30} + \frac{\sqrt{14}r}{3} + \frac{3\sqrt{30}r}{5} - \frac{8\sqrt{3}}{3} - \frac{3\sqrt{6}}{2} + \frac{31\sqrt{10}}{30} + \frac{2\sqrt{14}}{3} - \frac{3\sqrt{30}}{5} + 2\sqrt{10}cr + \frac{5909460810712307}{1125899906842624}$$

$$GA(G) = 12cr - 13r - 6c + \frac{2\sqrt{6}(8c-8)}{5} + \frac{2\sqrt{2}(2r+4)}{3} + \frac{\sqrt{15}(4r-4)}{4} + \frac{2\sqrt{30}(6r-6)}{11} + \frac{7295253401235797}{562949953421312}$$

$$H(G) = \frac{14c}{15} + \frac{73r}{198} + 2cr + \frac{26}{3465}$$

$$SC(G) = \frac{2r}{3} + \frac{\sqrt{2}(4c-6)}{4} + \frac{\sqrt{10}(8c-8)}{10} - \frac{\sqrt{3}(10c+13r-12cr-11)}{6} + \frac{\sqrt{2}(4r-4)}{4} + \frac{\sqrt{11}(6r-6)}{11} + \frac{15125962153204507}{3377699720527872}$$

$$B_1(G) = 384cr - 116r - 32c - 14$$

$$B_2(G) = 1440cr - 648r - 368c + 94$$

$$m_{B_1}(G) = \frac{949c}{1710} + \frac{339649r}{836940} + \frac{3cr}{5} + \frac{18270071}{76247380}$$

$$m_{B_2}(G) = \frac{5c}{12} + \frac{13r}{42} + \frac{2cr}{5} + \frac{113}{42}$$

$$HB(G) = \frac{949c}{855} + \frac{339649r}{418470} + \frac{6cr}{5} + \frac{18270071}{38123690}$$

Proof:

Using the M-polynomial obtained in Theorem 1, we define the various degree-based operator terms required for the expressions listed in Table 1, according to definitions (a). Consequently, the following results are obtained:

$$D_x(M) = 12x^3y^3 + 12x^3y^4 + (12r-12)x^3y^5 + (6r+12)x^3y^6 + (16c-24)x^4y^4 + (32c-32)x^4y^6 + (30r-30)x^5y^6 + (72cr-78r-60c+66)x^6y^6$$

$$D_y(M) = 12x^3y^3 + 16x^3y^4 + (20r-20)x^3y^5 + (12r+24)x^3y^6 + (16c-24)x^4y^4 + (48c-48)x^4y^6 + (36r-36)x^5y^6 + (72cr-78r-60c+66)x^6y^6$$

$$S_x(M)=\frac{4}{3}4x^3y^3+\frac{4}{3}x^3y^4+\frac{(4r-4)}{3}x^3y^5+\frac{(2r+4)}{3}x^3y^6+\frac{(4c-6)}{4}x^4y^4+\frac{(8c-8)}{4}x^4y^6+\frac{(6r-6)}{5}x^5y^6+\frac{(12cr-13r-10c+11)}{6}x^6y^6$$

$$S_y(M)=\frac{4}{3}4x^3y^3+\frac{4}{4}x^3y^4+\frac{(4r-4)}{5}x^3y^5+\frac{(2r+4)}{6}x^3y^6+\frac{(4c-6)}{4}x^4y^4+\frac{(8c-8)}{6}x^4y^6+\frac{(6r-6)}{6}x^5y^6+\frac{(12cr-13r-10c+11)}{6}x^6y^6$$

$$D_x^{\frac{-1}{2}}(M)=\frac{4}{\sqrt{3}}x^3y^3+\frac{4}{\sqrt{3}}x^3y^4+\frac{(4r-4)}{\sqrt{3}}x^3y^5+\frac{(2r+4)}{\sqrt{3}}x^3y^6+\frac{(4c-6)}{2}x^4y^4+\frac{(8c-8)}{2}x^4y^6+\frac{(6r-6)}{\sqrt{5}}x^5y^6+\frac{(12cr-13r-10c+11)}{\sqrt{6}}x^6y^6$$

$$D_y^{\frac{-1}{2}}(M)=\frac{4}{\sqrt{3}}x^3y^3+2x^3y^4+\frac{(4r-4)}{\sqrt{5}}x^3y^5+\frac{(2r+4)}{\sqrt{6}}x^3y^6+\frac{(4c-6)}{2}x^4y^4+\frac{(8c-8)}{\sqrt{6}}x^4y^6+\frac{(6r-6)}{\sqrt{6}}x^5y^6+\frac{(12cr-13r-10c+11)}{\sqrt{6}}x^6y^6$$

$$D_x^{2}(M)=36*4x^3y^3+36*4x^3y^4+36(4r-4)x^3y^5+36(2r+14)x^3y^6+64(4c-6)x^4y^4+64(8c-8)x^4y^6+100(6r-6)x^5y^6+144(12cr-13r-10c+11)x^6y^6$$

$$D_y^{2}(M)=36*4x^3y^3+64*4x^3y^4+100(4r-4)x^3y^5+144(2r+14)x^3y^6+64(4c-6)x^4y^4+144(8c-8)x^4y^6+144(6r-6)x^5y^6+144(12cr-13r-10c+11)x^6y^6$$

$$D_yS_x(M)=4x^3y^3+3x^3y^4+\frac{(12r-12)}{5}x^3y^5+(r+2)x^3y^6+(4c-6)x^4y^4+\frac{(16c-16)}{3}x^4y^6+(5r-5)x^5y^6+(12cr-13r-10c+11)x^6y^6$$

$$D_xS_y(M)=4x^3y^3+\frac{16}{3}x^3y^4+\frac{(20r-20)}{5}x^3y^5+(4r+8)x^3y^6+(4c-6)x^4y^4+(12c-12)x^4y^6+\frac{(36r-36)}{5}x^5y^6+(12cr-13r-10c+11)x^6y^6$$

$$J(M)=4x^6+4x^7+(4r+4c-10)x^8+(2r+4)x^9+(8c-8)x^{10}+(6r-6)x^{11}+(12cr-13r-10c+11)x^{12}$$

$$Q_{-2}J(M)=4x^4+4x^5+(4r+4c-10)x^6+(2r+4)x^7+(8c-8)x^8+(6r-6)x^9+(12cr-13r-10c+11)x^{10}$$

$$S_xJ(M)=\frac{4}{6}x^6+\frac{4}{7}x^7+\frac{(4r+4c-10)}{8}x^8+\frac{(2r+4)}{9}x^9+\frac{(8c-8)}{10}x^{10}+\frac{(6r-6)}{11}x^{11}+\frac{(12cr-13r-10c+11)}{12}x^{12}$$

$$S_x^{\frac{1}{2}}J(M)=\frac{4}{\sqrt{6}}x^6+\frac{4}{\sqrt{7}}x^7+\frac{(4r+4c-10)}{\sqrt{8}}x^8+\frac{(2r+4)}{\sqrt{9}}x^9+\frac{(8c-8)}{\sqrt{10}}x^{10}+\frac{(6r-6)}{\sqrt{11}}x^{11}+\frac{(12cr-13r-10c+11)}{\sqrt{12}}x^{12}$$

$$L_x(M)=4x^6y^3+4x^6y^4+(4r-4)x^6y^5+(2r+14)x^6y^6+(4c-6)x^8y^4+(8c-8)x^8y^6+(6r-6)x^{10}y^6+(12cr-13r-10c+11)x^{12}y^6$$

$$L_y(M)=4x^3y^6+4x^3y^8+(4r-4)x^3y^{10}+(2r+14)x^3y^{12}+(4c-6)x^4y^8+(8c-8)x^4y^{12}+(6r-6)x^5y^{12}+(12cr-13r-10c+11)x^6y^{12}$$

Using the defined operators listed in Table 1, we obtain the following:

$M_1(G) = (D_x + D_y)(M(G: x, y))|_{x=y=1} = 144cr - 40r - 80c - 6$

$M_2(G) = (D_x D_y)(M(G: x, y))|_{x=y=1} = 432cr - 192r - 104c + 24$

$M_2{}^m(G) = (S_x S_y)(M(G: x, y))|_{x=y=1} = \frac{11c}{36} + \frac{13r}{60} + \frac{cr}{3} + \frac{47}{360}$

$M_3(G) = |D_x - D_y|(M(G: x, y))|_{x=y=1} = 16c + 20r - 14=$

$$R(G) = \left(D_x^{\frac{-1}{2}} D_y^{\frac{-1}{2}}\right)(M(G: x, y))|_{x=y=1}$$

$$= 2cr - \frac{13r}{6} - \frac{2c}{3} + \frac{\sqrt{6}(8c - 8)}{12} + \frac{\sqrt{2}(2r + 4)}{6} + \frac{\sqrt{15}(4r - 4)}{15} + \frac{\sqrt{30}(6r - 6)}{30} + \frac{2382432804997525}{844424930131968}$$

$N_z(G) = |D_x{}^2 - D_y{}^2|(M(G: x, y))|_{x=y=1} = 160c + 184r - 154$

$$\chi_{\frac{1}{2}} N_z(G) = \sqrt{|D_x{}^2 - D_y{}^2|}(M(G: x, y))|_{x=y=1}$$

$$= 16r + 4\sqrt{7} + 2\sqrt{5}(8c - 8) + 3\sqrt{3}(2r + 4) + \sqrt{11}(6r - 6) - 16$$

$HM_1(G) = (D_x + D_y)^2(M(G: x, y))|_{x=y=1} = 1728cr - 728r - 384c + 82$

$\sigma(G) = (D_x - D_y)^2(M(G: x, y))|_{x=y=1} = 32c + 40r - 14$

$SDD(G) = (D_x S_y + D_y S_x)(M(G: x, y))|_{x=y=1} = \frac{16c}{3} + \frac{4r}{15} + 24cr - \frac{34}{15}$

$$ABC(G) = \left(\left(D_x^{\frac{-1}{2}} D_y^{\frac{-1}{2}}\right) * \left(D_x^{\frac{1}{2}} Q_{-2} J\right)\right)(M(G: x, y))|_{x=y=1}$$

$$= \frac{8\sqrt{3}c}{3} + \sqrt{6}c - \frac{5\sqrt{10}c}{3} - \frac{41\sqrt{10}r}{30} + \frac{\sqrt{14}r}{3} + \frac{3\sqrt{30}r}{5} - \frac{8\sqrt{3}}{3} - \frac{3\sqrt{6}}{2} + \frac{31\sqrt{10}}{30} + \frac{2\sqrt{14}}{3} - \frac{3\sqrt{30}}{5} + 2\sqrt{10}cr + \frac{5909460810712307}{1125899906842624}$$

$$GA(G) = \left(2\left(D_x^{\frac{1}{2}} D_y^{\frac{1}{2}}\right) * (S_x J)\right)(M(G: x, y))|_{x=y=1}$$

$$= 12cr - 13r - 6c + \frac{2\sqrt{6}(8c - 8)}{5} + \frac{2\sqrt{2}(2r + 4)}{3} + \frac{\sqrt{15}(4r - 4)}{4} + \frac{2\sqrt{30}(6r - 6)}{11} + \frac{7295253401235797}{562949953421312}$$

$H(G) = (2S_x J)(M(G: x, y))|_{x=y=1} = \frac{14c}{15} + \frac{73r}{198} + 2cr + \frac{26}{3465}$

$$SC(G) = \left(S_x^{\frac{1}{2}} J\right)(M(G: x, y))|_{x=y=1}$$

$$= \frac{2r}{3} + \frac{\sqrt{2}(4c - 6)}{4} + \frac{\sqrt{10}(8c - 8)}{10} - \frac{\sqrt{3}(10c + 13r - 12cr - 11)}{6} + \frac{\sqrt{2}(4r - 4)}{4} + \frac{\sqrt{11}(6r - 6)}{11} + \frac{15125962153204507}{3377699720527872}$$

$B_1(G) = ((D_x + D_y) + 2D_x Q_{-2} J))(M(G: x, y))|_{x=y=1} = 384cr - 116r - 32c - 14$

$B_2(G) = (D_x Q_{-2} J(D_x + D_y))(M(G: x, y))|_{x=y=1} = 1440cr - 648r - 368c + 94$

$m_{B_1}(G) = \left(S_x Q_{-2} J(L_x + L_y)\right)(M(G: x, y))|_{x=y=1} = \frac{949c}{1710} + \frac{339649r}{836940} + \frac{3cr}{5} + \frac{18270071}{76247380}$

$$m_{B_2}(G) = \left(S_x Q_{-2} J(S_x + S_y)\right)\left(M(G: x, y)\right)|_{x=y=1} = \frac{5c}{12} + \frac{13r}{42} + \frac{2cr}{5} + \frac{113}{42}$$

$$HB(G) = \left(2S_x Q_{-2} J(L_x + L_y)\right)\left(M(G: x, y)\right)|_{x=y=1}$$
$$= \frac{949c}{855} + \frac{339649r}{418470} + \frac{6cr}{5} + \frac{18270071}{38123690}$$

3.2. S_2 Borophene structure.

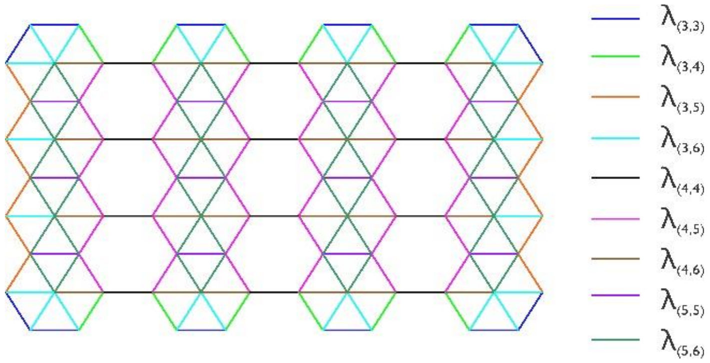

Figure 3. Edge partition of S_2 borophene structure.

Theorem 3: Let $G = S_2(r, c)$ such that $r, c \geq 1$ be the connectivity graph of the S_2-borophene nanosheet as shown in the figure, then the M-polynomial is defined to be:

$$M(G; x, y) = (2c+4)x^3y^3 + (4c-4)x^3y^4 + (4r-4)x^3y^5 + (4c+2r)x^3y^6 + (cr-r)x^4y^4 + 4(r-1)(c-1)x^4y^5 + (2cr-2r)x^4y^6 + (cr-c)x^5y^5 + (4cr-4c)x^5y^6$$

Proof:

Consider the connectivity graph $G = S_2(r, c)$; $r, c \geq 1$ with $|V(G)| = 5cr + 2r$ and $|E(G)| = (12c-1)r + c$. The partition of the edge set based on the vertex degree is given by $\lambda_{(k,l)} = \{(a, b) \epsilon E(G): d_a = k, d_b = l\}$. The connectivity graph of the S_2-Borophene nanosheet is illustrated in Figure 3, and the corresponding M-polynomial representation is shown in Figure 4. It is observed that:

Edge partition	$\lambda_{(3,3)}$	$\lambda_{(3,4)}$	$\lambda_{(3,5)}$	$\lambda_{(3,6)}$	$\lambda_{(4,4)}$	$\lambda_{(4,5)}$	$\lambda_{(4,6)}$	$\lambda_{(5,5)}$	$\lambda_{(5,6)}$
Cardinality	$2c+4$	$4c-4$	$4r-4$	$4c+2r$	$cr-r$	$4(r-1)(c-1)$	$2cr-2r$	$cr-c$	$4cr-4c$

By the definition of the M-polynomial, we get:

$$M(G; x, y) = |\lambda_{(3,3)}|x^3y^3 + |\lambda_{(3,4)}|x^3y^4 + |\lambda_{(3,5)}|x^3y^5 + |\lambda_{(3,6)}|x^3y^6 + |\lambda_{(4,4)}|x^4y^4 + |\lambda_{(4,5)}|x^4y^5 + |\lambda_{(4,6)}|x^4y^6 + |\lambda_{(5,5)}|x^5y^5 + |\lambda_{(5,6)}|x^5y^6$$
$$= (2c+4)x^3y^3 + (4c-4)x^3y^4 + (4r-4)x^3y^5 + (4c+2r)x^3y^6 + (cr-r)x^4y^4 + 4(r-1)(c-1)x^4y^5 + (2cr-2r)x^4y^6 + (cr-c)x^5y^5 + (4cr-4c)x^5y^6$$

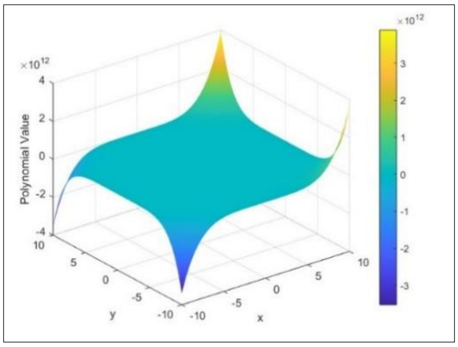

Figure 4. Graphical Representation of the M-polynomial for S_2 borophene structure.

Theorem 4: For $G = S_2(r,c)$ such that $r, c \geq 1$,

$$M_1(G) = 118cr - 14r - 14c$$

$$M_2(G) = 289cr - 48r - 87c + 8$$

$$M_2^{\,m}(G) = \frac{91c}{225} + \frac{23r}{720} + \frac{623cr}{1200} + \frac{2}{45}$$

$$M_3(G) = 8c + 6r + 12cr - 8$$

$$R(G) = \frac{7c}{15} - \frac{r}{4} - \frac{\sqrt{30}(4c - 4cr)}{30} - \frac{\sqrt{6}(2r - 2cr)}{12} + \frac{9cr}{20} + \frac{\sqrt{2}(4c + 2r)}{6} + \frac{\sqrt{3}(4c - 4)}{6} + \frac{\sqrt{15}(4r - 4)}{15} + \frac{\sqrt{5}(4r - 4)(c - 1)}{10} + \frac{4}{3}$$

$$N_z(G) = 56c + 42r + 120cr - 56$$

$$\chi_{\frac{1}{2}}N_z(G) = 16r - \sqrt{11}(4c - 4cr) - 2\sqrt{5}(2r - 2cr) + 3(4r - 4)(c - 1) + 3\sqrt{3}(4c + 2r) + \sqrt{7}(4c - 4) - 16$$

$$HM_1(G) = 1172cr - 170r - 316c + 16$$

$$\sigma(G) = 32c + 22r + 16cr - 16$$

$$SDD(G) = 4c - \frac{7r}{15} + \frac{74cr}{3} - \frac{6}{5}$$

$$ABC(G) = \frac{4c}{3} + \sqrt{14}\left(\frac{2c}{3} + \frac{r}{3}\right) + \sqrt{15}\left(\frac{2c}{3} - \frac{2}{3}\right) + \sqrt{10}\left(\frac{4r}{5} - \frac{4}{5}\right) + \frac{\sqrt{35}(4r - 4)(c - 1)}{10} + \frac{2\sqrt{2}c(r - 1)}{5} + \frac{2\sqrt{3}r(c - 1)}{3} + \frac{\sqrt{6}r(c - 1)}{4} + \frac{2\sqrt{30}c(r - 1)}{5} + \frac{8}{3}$$

$$GA(G) = c - r - \frac{2\sqrt{30}(4c - 4cr)}{11} - \frac{2\sqrt{6}(2r - 2cr)}{5} + 2cr + \frac{2\sqrt{2}(4c + 2r)}{3} + \frac{4\sqrt{3}(4c - 4)}{7} + \frac{\sqrt{15}(4r - 4)}{4} + \frac{4\sqrt{5}(4r - 4)(c - 1)}{9} + 4$$

$$H(G) = \frac{1019c}{1155} - \frac{17r}{180} + \frac{4883cr}{1980} + \frac{5}{63}$$

$$SC(G) = \frac{\sqrt{6}c}{3} - \frac{2r}{3} + \frac{4\sqrt{7}c}{7} - \frac{\sqrt{10}c}{10} - \frac{4\sqrt{11}c}{11} + \frac{3\sqrt{2}r}{4} - \frac{\sqrt{10}r}{5} + \frac{4cr}{3} - \sqrt{2} + \frac{2\sqrt{6}}{3} - \frac{4\sqrt{7}}{7} + \frac{\sqrt{2}cr}{4} + \frac{3\sqrt{10}cr}{10} + \frac{4\sqrt{11}cr}{11} + \frac{4}{3}$$

$$B_1(G) = 306cr - 38r - 46c$$

$$B_2(G) = 936cr - 142r - 288c + 16$$

$$m_{B_1}(G) = \frac{69702842617c}{93669906330} + \frac{179297r}{2467530} + \frac{6324586cr}{6769035} + \frac{452477}{6235515}$$

$$m_{B_2}(G) = \frac{2327c}{3780} + \frac{271r}{5040} + \frac{9943cr}{15120} + \frac{32}{315}$$

$$HB(G) = \frac{69702842617c}{46834953165} + \frac{179297r}{1233765} + \frac{12649172cr}{6769035} + \frac{904954}{6235515}$$

Proof:

Similar to proof of Theorem 2.

3.3. S_3 Borophene structure.

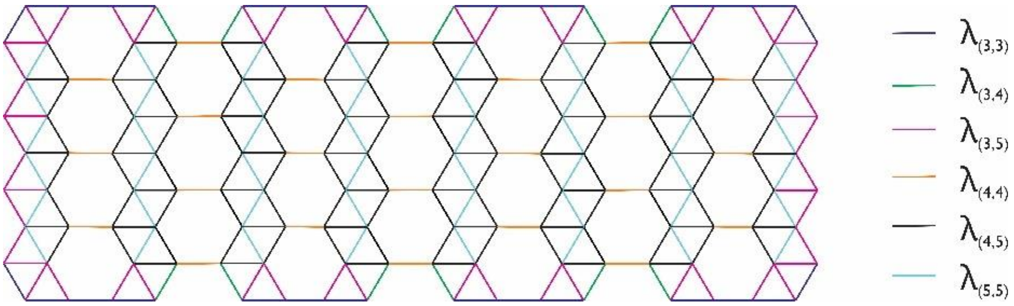

Figure 5. Edge partition of S_3 borophene structure.

Theorem 5: Let $G = S_3(r,c)$ such that $r,c \geq 1$ be the connectivity graph of the S_3-borophene nanosheet, as shown in the figure, then the M-polynomial is defined to be:

$$M(G;x,y) = (6c+4)x^3y^3 + (4c-4)x^3y^4 + (6r+8c-4)x^3y^5 + (2rc-r-c)x^4y^4 + (12cr-10c-6r+4)x^4y^5 + (4cr-4c)x^5y^5$$

Proof:

Consider the connectivity graph $G = S_3(r,c)\,;\, r,c \geq 1$ with $|V(G)| = 8cr + 4c$ and $|E(G)| = 18cr - r + 3c$. The partition of the edge set based on the vertex degree is given by $\lambda_{(k,l)} = \{(a,b)\, \epsilon\, E(G): d_a = k, d_b = l\}$. The connectivity graph of the S_3-Borophene nanosheet is illustrated in Figure 5, and the corresponding M-polynomial representation is shown in Figure 6. It is observed that:

Edge partition	$\lambda_{(3,3)}$	$\lambda_{(3,4)}$	$\lambda_{(3,5)}$	$\lambda_{(4,4)}$	$\lambda_{(4,5)}$	$\lambda_{(5,5)}$
Cardinality	6*c*+4	4*c*-4	6*r*+8*c*-4	2*cr*-*r*-*c*	12*cr*-10*c*-6*r*+4	4*cr*-4*c*

By the definition of the M-polynomial, we get,

$$M(G;x,y) = |\lambda_{(3,3)}|x^3y^3 + |\lambda_{(3,4)}|x^3y^4 + |\lambda_{(3,5)}|x^3y^5 + |\lambda_{(4,4)}|x^4y^4 + |\lambda_{(4,5)}|x^4y^5 + |\lambda_{(5,5)}|x^5y^5$$

$$= (6c+4)x^3y^3 + (4c-4)x^3y^4 + (6r+8c-4)x^3y^5 + (2cr-r-c)x^4y^4 + (12cr-10c+6r+4)x^4y^5 + (4cr-4c)x^5y^5$$

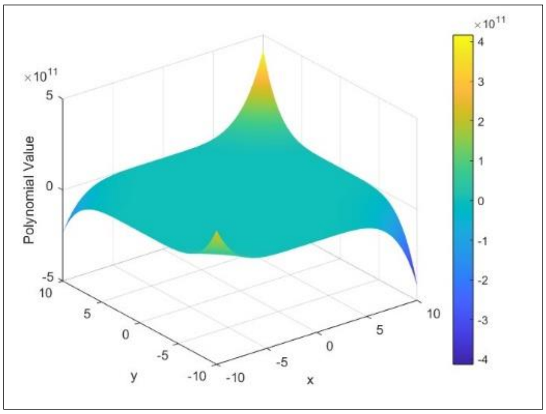

Figure 6. Graphical representation of the M-polynomial for S_3 borophene structure.

Theorem 6: For $G = S_3(r,c)$ such that $r,c \geq 1$,

$$M_1(G) = 164cr - 14r - 10c$$

$$M_2(G) = 372cr - 46r - 94c + 8$$

$$M_2^{\,m}(G) = \frac{973c}{1200} + \frac{3r}{80} + \frac{177cr}{200} + \frac{2}{45}$$

$$M_3(G) = 10c + 6r + 12cr - 8$$

$$R(G) = \frac{19c}{20} - \frac{r}{4} + \frac{13cr}{10} + \frac{\sqrt{15}(8c + 6r - 4)}{15} + \frac{\sqrt{3}(4c - 4)}{6} - \frac{\sqrt{5}(10c + 6r - 12cr - 4)}{10} + \frac{4}{3}$$

$$N_z(G) = -56 + 42r + 108cr + 66c$$

$$\chi_{\frac{1}{2}}N_z(G) = 2c + 6r + 36cr + \sqrt{7}(4c - 4) - 4$$

$$HM_1(G) = 1500cr - 166r - 350c + 16$$

$$\sigma(G) = 26c + 18r + 12cr - 16$$

$$SDD(G) = \frac{239c}{30} - \frac{7r}{10} + \frac{183cr}{5} - \frac{6}{5}$$

$$ABC(G) = 4c - \frac{2\sqrt{2}}{5}(4c - 4cr) + \frac{\sqrt{10}}{5}(8c + 6r - 4) + \frac{\sqrt{15}}{6}(4c - 4) - \frac{\sqrt{35}}{10}(10c + 6r - 12cr - 4) - \frac{\sqrt{6}}{4}(c + r - 2cr) + \frac{8}{3}$$

$$GA(G) = c - r + 6cr + \frac{\sqrt{15}}{4}(8c + 6r - 4) + \frac{4\sqrt{3}}{7}(4c - 4) - \frac{4\sqrt{5}}{9}(10c + 6r - 12cr - 4) + 4$$

$$H(G) = \frac{1019r}{1155} - \frac{17c}{180} + \frac{4883cr}{1980} + \frac{5}{63}\{\text{Citation}\}$$

$$SC(G) = \frac{7\sqrt{2}}{4}c - 2r - \frac{10c}{3} + \sqrt{6}c + \frac{4\sqrt{7}}{7}c - \frac{2\sqrt{10}}{5}c + \frac{5\sqrt{2}}{4}r + 4cr - \sqrt{2} + \frac{2\sqrt{6}}{3} - \frac{4\sqrt{7}}{7}(4 + \frac{\sqrt{2}}{2}cr + \frac{2\sqrt{10}}{5}cr + \frac{4}{3}$$

$$B_1(G) = 420cr - 38r - 42c$$

$$B_2(G) = 1172cr - 138r - 330c + 16$$

$$m_{B_1}(G) = \frac{64590241c}{43648605} + \frac{121r}{1482} + \frac{632cr}{399} + \frac{452477}{6235515}$$

$$m_{B_2}(G) = \frac{1577c}{1260} + \frac{9r}{140} + \frac{239cr}{210} + \frac{32}{315}$$

$$HB(G) = \frac{129180482c}{43648605} + \frac{121r}{741} + \frac{1264cr}{399} + \frac{904954}{6235515}$$

Proof:

Similar to proof of Theorem 2.

3.4. S_4 borophene structure.

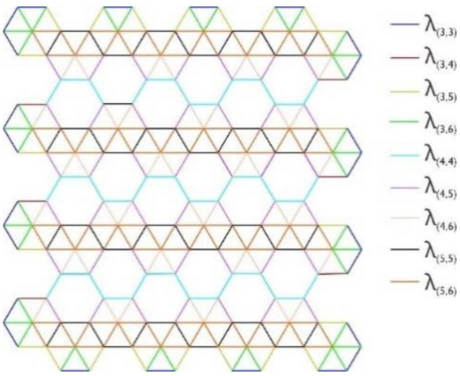

Figure 7. Edge partition of S_4 borophene structure.

Theorem 7: Let $G = S_4(r,c)$ such that $r,c \geq 1$ be the connectivity graph of the S_4-borophene nanosheet as shown in the figure, then the M-polynomial is defined to be:

$$M(G;x,y) = (4r+2c)x^3y^3 + (2r-2)x^3y^4 + (2r+4c-2)x^3y^5 + (6r+4c-2)x^3y^6 + (4cr-3r-4c+3)x^4y^4 + (4cr-2r-4c+2)x^4y^5 + (4cr-2r-4c+2)x^4y^6 + (4cr-3r)x^5y^5 + (8cr-4r)x^5y^6$$

Proof:

Consider the connectivity graph $G = S_4(r,c)\,; r,c \geq 1$ with $|V(G)| = 10cr + 2r$ and $|E(G)| = 24cr - 2c + 1$. The partition of the edge set based on the vertex degree is given by $\lambda_{(k,l)} = \{(a,b)\,\epsilon\, E(G): d_a = k, d_b = l\}$. The connectivity graph of the S_4-borophene nanosheet is illustrated in Figure 7 and the corresponding M-polynomial representation is shown in Figure 8. It is observed that:

Edge partition	$\lambda_{(3,3)}$	$\lambda_{(3,4)}$	$\lambda_{(3,5)}$	$\lambda_{(3,6)}$	$\lambda_{(4,4)}$	$\lambda_{(4,5)}$	$\lambda_{(4,6)}$	$\lambda_{(5,5)}$	$\lambda_{(5,6)}$
Cardinality	$4r+2c$	$2r-2$	$2r+4c-2$	$6r+4c-2$	$4cr-3r-4c+3$	$4cr-2r-4c+2$	$4cr-2r-4c+2$	$4cr-3r$	$8cr-4r$

By the definition of the M-polynomial, we get,

$$\begin{aligned} M(G;x,y) &= |\lambda_{(3,3)}|x^3y^3 + |\lambda_{(3,4)}|x^3y^4 + |\lambda_{(3,5)}|x^3y^5 + |\lambda_{(3,6)}|x^3y^6 + |\lambda_{(4,4)}|x^4y^4 \\ &\quad + |\lambda_{(4,5)}|x^4y^5 + |\lambda_{(4,6)}|x^4y^6 + |\lambda_{(5,5)}|x^5y^5 + |\lambda_{(5,6)}|x^5y^6 \\ &= (4r+2c)x^3y^3 + (2r-2)x^3y^4 + (2r+4c-2)x^3y^5 \\ &\quad + (6r+4c-2)x^3y^6 + (4cr-3r-4c+3)x^4y^4 \\ &\quad + (4cr-2r-4c+2)x^4y^5 + (4cr-2r-4c+2)x^4y^6 \\ &\quad + (4cr-3r)x^5y^5 + (8cr-4r)x^5y^6 \end{aligned}$$

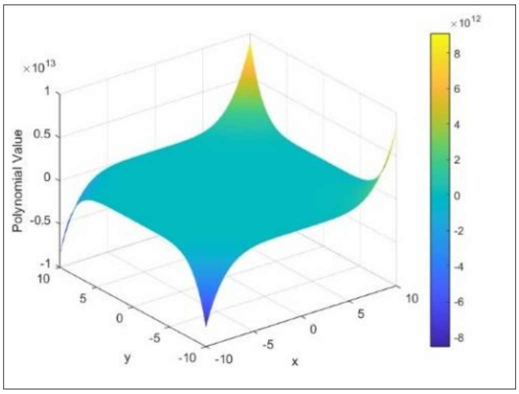

Figure 8. Graphical representation of the M-polynomial for S_4 borophene structure.

Theorem 8: For $G = S_4(r,c)$ such that $r,c \geq 1$,

$$M_1(G) = 236cr - 28r - 28c + 14$$

$$M_2(G) = 580cr - 133r - 90c + 46$$

$$M_2{}^m(G) = \frac{17c}{180} + \frac{1633r}{3600} + \frac{313cr}{300} - \frac{29}{720}$$

$$M_3(G) = 8c + 14r + 20cr - 6$$

$$R(G) = \frac{9cr}{5} - \frac{r}{60} - \frac{\sqrt{30}(4r - 8cr)}{30} - \frac{c}{3} + \frac{\sqrt{2}(4c + 6r - 2)}{6} + \frac{\sqrt{15}(4c + 2r - 2)}{15} - \frac{\sqrt{5}(4c + 2r - 4cr - 2)}{10} - \frac{\sqrt{6}(4c + 2r - 4cr - 2)}{12} + \frac{\sqrt{3}(2r - 2)}{6} + \frac{3}{4}$$

$$N_z(G) = -42 + 106r + 204cr + 56c$$

$$\chi_{\frac{1}{2}}N_z(G) = 4c + 2r - \sqrt{11}(4r - 8cr) + 12cr + 3\sqrt{3}(4c + 6r - 2) - 2\sqrt{5}(4c + 2r - 4cr - 2) + \sqrt{7}(2r - 2) - 2$$

$$HM_1(G) = 2348cr - 482r - 328c + 166$$

$$\sigma(G) = 32c + 50r + 28cr - 18$$

$$SDD(G) = \frac{47r}{15} - \frac{9c}{5} + \frac{737cr}{15} + \frac{11}{15}$$

$$ABC(G) = \frac{4c}{3} + \frac{8r}{3} - \frac{2\sqrt{2}(3r - 4cr)}{5} - \frac{\sqrt{3}(4c + 2r - 4cr - 2)}{3} + \frac{\sqrt{10}(4c + 2r - 2)}{5} + \frac{\sqrt{14}(4c + 6r - 2)}{6} - \frac{\sqrt{6}(4c + 3r - 4cr - 3)}{4} - \frac{\sqrt{35}(4c + 2r - 4cr - 2)}{10} + \frac{\sqrt{15}(2r - 2)}{6} - \frac{\sqrt{30}(4r - 8cr)}{10}$$

$$GA(G) = 8cr - 2r - \frac{2\sqrt{30}(4r - 8cr)}{11} - 2c + \frac{2\sqrt{2}(4c + 6r - 2)}{3} + \frac{15^{\frac{1}{2}} * (4 * c + 2 * r - 2)}{4} - \frac{4\sqrt{5}(4c + 2r - 4cr - 2)}{9} - \frac{2\sqrt{6}(4c + 2r - 4cr - 2)}{5} + \frac{4\sqrt{3}(2r - 2)}{7} + 3$$

$$H(G) = \frac{2263r}{2772} - \frac{2c}{15} + \frac{2447cr}{495} + \frac{11}{140}$$

$$SC(G) = \frac{4r}{3} + \frac{\sqrt{6}c}{3} - \frac{2\sqrt{10}c}{5} - \frac{\sqrt{2}r}{4} + \frac{2\sqrt{6}r}{3} + \frac{2\sqrt{7}r}{7} - \frac{\sqrt{10}r}{2} - \frac{4\sqrt{11}r}{11} + \frac{4cr}{3} + \frac{\sqrt{2}}{4} - \frac{2\sqrt{7}}{7} + \frac{\sqrt{10}}{5} + \sqrt{2}cr + \frac{4\sqrt{10}cr}{5} + \frac{8\sqrt{11}cr}{11}$$

$$B_1(G) = 612cr - 84r - 76c + 38$$

$$B_2(G) = 1876cr - 426r - 272c + 138$$

$$m_{B_1}(G) = \frac{240088c}{1233765} + \frac{79307744291r}{93669906330} + \frac{12692527cr}{6769035} - \frac{19761362}{230714055}$$

$$m_{B_2}(G) = \frac{443c}{2520} + \frac{307r}{432} + \frac{2003cr}{1512} - \frac{359}{5040}$$

$$HB(G) = \frac{480176c}{1233765} + \frac{79307744291r}{46834953165} + \frac{25385054cr}{6769035} - \frac{39522724}{230714055}$$

Proof:

Similar to proof of Theorem 2.

3.5. S_5 borophene structure.

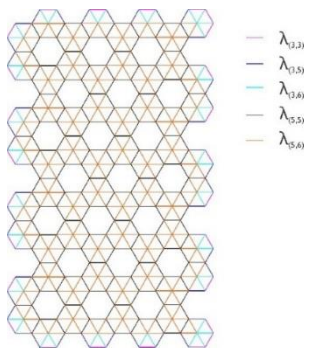

Figure 9. Edge partition of S_5 borophene structure.

Theorem 9: Let $G = S_5(r,c)$ such that $r,c \geq 1$ be the connectivity graph of the S_5-borophene nanosheet, as shown in the figure, then the M-polynomial is defined to be:

$$M(G;x,y) = (4r+2c+2)x^3y^3 + (8r+4c-2)x^3y^5 + (8r+4c)x^3y^6 + (18cr-10r-5c+2)x^5y^5 + (24cr-8r-4c)x^5y^6$$

Proof:

Consider the connectivity graph $G = S_5(r,c)\,;\, r,c \geq 1$ with $|V(G)| = 16cr+4r+2c$ and $|E(G)| = 42cr+c+2r$. The partition of the edge set based on the vertex degree is given by $\lambda_{(k,l)} = \{(a,b)\,\epsilon\, E(G){:}\, d_a = k, d_b = l\}$. The connectivity graph of the S_5-borophene nanosheet is illustrated in Figure 9 and the corresponding M-polynomial representation is shown in Figure 10. It is observed that:

Edge partition	$\lambda_{(3,3)}$	$\lambda_{(3,5)}$	$\lambda_{(3,6)}$	$\lambda_{(5,5)}$	$\lambda_{(5,6)}$
Cardinality	$4r+2c+2$	$8r+4c-2$	$8r+4c$	$18cr-10r-5c+2$	$24cr-8r-4c$

By the definition of the M-polynomial, we get,

$$M(G;x,y) = |\lambda_{(3,3)}|x^3y^3 + |\lambda_{(3,5)}|x^3y^5 + |\lambda_{(3,6)}|x^3y^6 + |\lambda_{(5,5)}|x^5y^5 + |\lambda_{(5,6)}|x^5y^6$$
$$= (4r+2c+2)x^3y^3 + (8r+4c-2)x^3y^5 + (8r+4c)x^3y^6 + (18cr-10r-5c+2)x^5y^5 + (24cr-8r-4c)x^5y^6$$

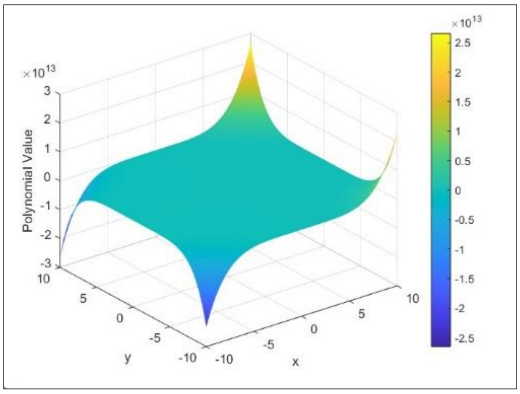

Figure 10. Graphical representation of the M-polynomial for S_5 borophene structure.

Theorem 10: For $G = S_5(r,c)$ such that $r,c \geq 1$,

$$M_1(G) = 444cr - 28r - 14c + 16$$
$$M_2(G) = 1170cr - 190r - 95c + 38$$
$$M_2{}^m(G) = \frac{17c}{45} + \frac{34r}{45} + \frac{38cr}{25} + \frac{38}{225}$$
$$M_3(G) = 16c + 32r + 24cr - 4$$
$$R(G) = \frac{18cr}{5} - \frac{2r}{3} - \frac{c}{3} + \frac{\sqrt{2}(4c+8r)}{6} + \frac{\sqrt{15}(4c+8r-2)}{15} - \frac{\sqrt{30}(4c+8r-24cr)}{30} + \frac{16}{15}$$
$$N_z(G) = 128c + 256r + 264cr - 32$$
$$\chi_{\frac{1}{2}}N_z(G) = 16c + 32r + 3\sqrt{3}(4c+8r) - \sqrt{11}(4c+8r-24cr) - 8$$
$$HM_1(G) = 4704cr - 664r - 332c + 144$$
$$\sigma(G) = 48c + 96r + 24cr - 8$$
$$SDD(G) = \frac{74c}{15} + \frac{148r}{15} + \frac{424cr}{5} + \frac{52}{15}$$

$$ABC(G) = \frac{4c}{3} + \frac{8r}{3} - \frac{2\sqrt{2}(5c + 10r - 18cr - 2)}{5} + \frac{\sqrt{10}(4c + 8r - 2)}{5} + \frac{\sqrt{14}(4c + 8r)}{6} - \frac{\sqrt{30}(4c + 8r - 24cr)}{10} + \frac{4}{3}$$

$$GA(G) = 18cr - 6r - 3c + \frac{2\sqrt{2}(4c + 8r)}{3} + \frac{\sqrt{15}(4c + 8r - 2)}{4} - \frac{2\sqrt{30}(4c + 8r - 24cr)}{11} + 4$$

$$H(G) = \frac{82c}{99} + \frac{164r}{99} + \frac{438cr}{55} + \frac{17}{30}$$

$$SC(G) = \frac{4c}{3} + \frac{8r}{3} + \frac{\sqrt{6}(2c + 4r + 2)}{6} + \frac{\sqrt{2}(4c + 8r - 2)}{4} - \frac{\sqrt{10}(5c + 10r - 18cr - 2)}{10} - \frac{\sqrt{11}(4c + 8r - 24cr)}{11}$$

$$B_1(G) = 1164cr - 92r - 46c + 40$$

$$B_2(G) = 3816cr - 608r - 304c + 112$$

$$m_{B_1}(G) = \frac{688717c}{976430} + \frac{688717r}{488215} + \frac{7201cr}{2639} + \frac{817}{2730}$$

$$m_{B_2}(G) = \frac{2123c}{3780} + \frac{2123r}{1890} + \frac{169cr}{90} + \frac{23}{90}$$

$$HB(G) = \frac{688717c}{488215} + \frac{1377434r}{488215} + \frac{14402cr}{2639} + \frac{817}{1365}$$

Proof:

Similar to proof of Theorem 2.

4. Quantitative Structure Property Relationship

Of all the values, the numerical values corresponding to $r = 4$ and $c = 4$ for each of the degree-based descriptors of the Borophene sheet are considered for further study, as this combination represents the complete structural configuration of the sheet and captures the dominant degree interactions present in the lattice. These values also provide a comprehensive and representative characterization of the underlying structure, making it suitable for subsequent correlation and analysis. Further, the mechanical properties such as Young's modulus (Y), Poisson's ratio (P), strain at ultimate tensile strength (STS), and ultimate tensile strength (UTS) are considered. The values of Y, P, STS, and UTS [28] are given in Table 2.

Table 2. Mechanical properties of S_{1-5} borophene structure.

	Y	P	STS	UTS
S_1	382	-0.010	0.105	22.80
S_2	190	+0.018	0.200	19.97
S_3	208	+0.110	0.210	19.91
S_4	186	+0.260	0.140	15.65
S_5	214	+0.200	0.210	14.84

The correlation coefficient (R) between the mechanical properties and the degree-based topological indices of the Borophene nanosheets for $r = 4$ and $c = 4$ is calculated and given in Table 3. Based on the correlation coefficient (R), it is found that the third Zagreb index $M_3(G)$ is the best fit for the Young's modulus (Y), Sigma index $\sigma(G)$ for Poisson's ratio (P), Modified Second-k Banhatti index $m_{B_2}(G)$ for strain at ultimate tensile strength (STS) and Sigma index $\sigma(G)$ for Ultimate tensile strength (UTS).

Table 3. Correlation coefficient (R).

	Y	P	STS	UTS
$M_1(G)$	-0.254	0.669	0.342	-0.810
$M_2(G)$	-0.171	0.615	0.280	-0.768
${M_2}^m(G)$	-0.516	0.806	0.533	-0.884
$M_3(G)$	**-0.560**	0.822	0.447	-0.961
$R(G)$	-0.426	0.766	0.471	-0.872
$N_z(G)$	-0.517	0.798	0.410	-0.950
$\chi_{\frac{1}{2}}N_z(G)$	-0.539	0.794	0.479	-0.941
$HM_1(G)$	-0.176	0.619	0.280	-0.771
$\sigma(G)$	-0.525	**0.823**	0.308	**-0.965**
$SDD(G)$	-0.345	0.724	0.406	-0.851
$ABC(G)$	-0.370	0.737	0.430	-0.857
$GA(G)$	-0.335	0.716	0.406	-0.843
$H(G)$	-0.424	0.765	0.471	-0.870
$SC(G)$	-0.380	0.742	0.438	-0.859
$B_1(G)$	-0.241	0.661	0.332	-0.805
$B_2(G)$	-0.158	0.607	0.266	-0.761
$m_{B_1}(G)$	-0.516	0.806	0.532	-0.885
$m_{B_2}(G)$	-0.540	0.814	**0.550**	-0.883
$HB(G)$	-0.516	0.806	0.532	-0.885

Further regression models are employed to model the respective curves. Accordingly, the regression models investigated in this work comprise linear, quadratic, cubic, exponential, and logarithmic models, as depicted in Figure 11. Owing to the limited number of borophene structures available, statistical indicators are treated with caution, with the primary focus on goodness-of-fit rather than predictive generalization. The coefficient of determination (R2) for the investigated regression models is presented in Table 4 and measures the proportion of variance in the mechanical property accounted for by the corresponding DBTI. A higher R^2 value signifies a better correlation and goodness of fit. For a specific mechanical property, the TI with the highest R^2 value is thus identified as the most reliable predictor of the respective dependent variable. Besides R^2, the mean absolute error (MAE) and root mean square error (RMSE) are also presented in Table 4. They are used to evaluate the predictive capability of the regression models. MAE provides a direct assessment of the average absolute difference between predicted and actual values, whereas RMSE emphasizes larger differences and reflects the overall robustness of the regression fit. Therefore, a combination of a higher R^2 value and lower MAE and RMSE values indicates better predictive reliability of the proposed models.

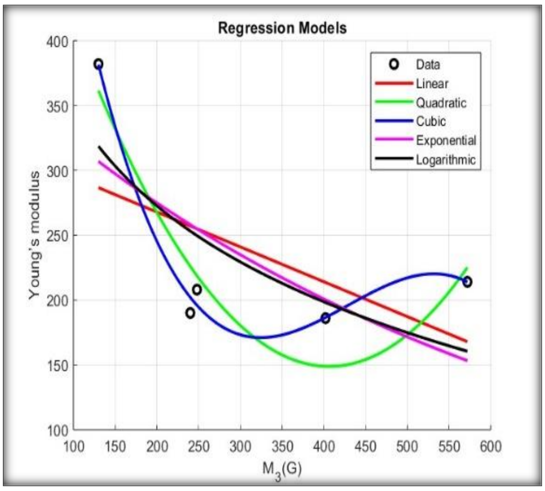

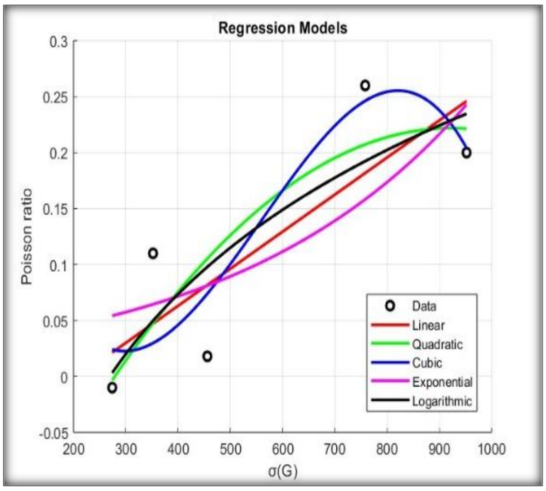

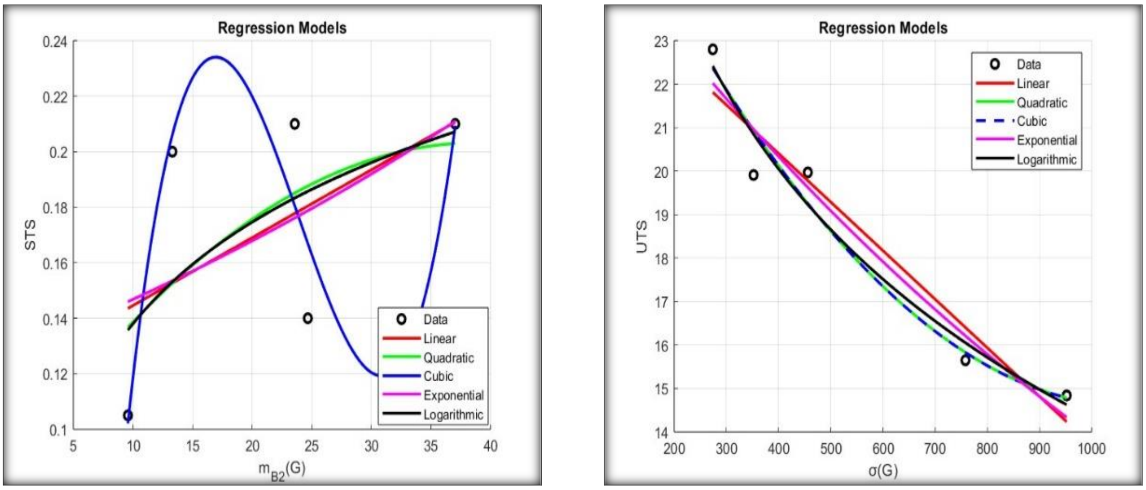

Figure 11. Regression models.

Table 4. Performance metrics.

Regression Model	MAE	RMSE	R^2
		$Y\ vs\ M_3(G)$	
Linear	56.610	61.128	0.313
Quadratic	23.059	25.792	0.878
Cubic	**05.011**	**07.634**	**0.989**
Exponential	53.025	57.248	0.398
Logarithmic	46.774	50.512	0.531
		$P\ vs\ \sigma(G)$	
Linear	0.056	0.059	0.677
Quadratic	0.046	0.054	0.722
Cubic	**0.038**	**0.047**	**0.795**
Exponential	0.064	0.067	0.580
Logarithmic	0.051	0.057	0.701
		$STS\ vs\ m_{B_2}(G)$	
Linear	0.032	0.036	0.303
Quadratic	0.032	0.035	0.326
Cubic	**0.013**	**0.018**	**0.821**
Exponential	0.032	0.036	0.293
Logarithmic	0.031	0.035	0.351
		$UTS\ vs\ \sigma(G)$	
Linear	0.714	0.776	0.932
Quadratic	0.482	0.598	0.959
Cubic	**0.481**	**0.598**	**0.959**
Exponential	0.647	0.692	0.946
Logarithmic	0.536	0.597	0.959

5. Results and Discussion

On comparing all the MAE, RSME, and R^2 values, it can be seen that the cubic regression model represents a better fit for all the given datasets. Thus, we have the regression equations as follows:

Young's modulus(Y) vs Third Zagreb index ($M_3(G)$)

$$Y = -1 * 10^{-5}(M_3(G))^{3} + 0.0142(M_3(G))^{2} - 5.7079(M_3(G)) + 908.51$$

Poisson ratio (P) vs Sigma index (σ(G))

$$P = -3 * 10^{-9}(\sigma(G))^3 + 5 * 10^{-6}(\sigma(G))^2 - 0.0024(\sigma(G)) + 0.3329$$

STS vs Modified Second-k Banhatti index ($m_{B_2}(G)$)

$$STS = 9 * 10^{-5}(m_{B_2}(G))^3 - 0.0062(m_{B_2}(G))^2 + 0.1349(m_{B_2}(G)) - 0.6997$$

UTS vs Sigma index (σ(G))

$$\mathrm{UTS} = 4 * 10^{-10}(\sigma(G))^3 + 1 * 10^{-5}(\sigma(G))^2 - 0.0255(\sigma(G)) + 28.493$$

6. Conclusions

This work introduces a new and integrative methodology to explain the mechanical performance of borophene nanosheets using mathematical graph theory. Using degree-based topological indices derived from the M-polynomial, we have established a semi-quantitative model that effectively relates the structural properties of borophene to its mechanical behavior. The examination of various topological indices reveals distinct predictive abilities for different mechanical parameters. The findings of the correlation indicate that the different mechanical properties are best represented by a single variable. That is, the third Zagreb index has the highest correlation with Young's modulus; the Sigma index is the superior predictor for Poisson's ratio and ultimate tensile strength, while the modified second-k Banhatti index exhibits the strongest correlation with strain at ultimate tensile strength. Regression analysis further supports the wholesomeness of this approach. Among the models tested, the cubic regression presented the highest coefficient of determination (R^2). It shows that the relationship between the topological indices and borophene's mechanical properties is nonlinear. Thus, modeling with higher orders is more appropriate for capturing it.

This study bridges a considerable gap between material science and theoretical chemistry by combining computational mechanical modeling with graph-theoretical descriptors. The methodology used allows efficient prediction of mechanical properties without relying on extensive atomistic simulations. It further offers a systematic way to understand the structure-property relationships arising in the 2D materials. Although the current analysis is based on a small number of borophene nanosheets due to the nascent state of the field, the proposed method provides a useful framework that can be easily expanded as more experimental data become available. Thus, this work provides a comprehensive framework for describing borophene nanosheets using TI and demonstrates their effectiveness in capturing mechanical behavior. The results demonstrate the strength of interdisciplinary advances in driving material discovery and design.

Author Contributions

Conceptualization, D.K.V.; methodology, K.B.R.; software, K.B.R.; validation, D.K.V.; formal analysis, S.; investigation, S.A.S.; project administration, S.A.S.; supervision, S.; visualization, S.A.S.; data curation, D.K.V.; writing—original draft preparation, D.K.V.; writing—review and editing, S.A.S. All authors have read and agreed to the published version of the manuscript.

Institutional Review Board Statement

Not applicable.

Informed Consent Statement

Not applicable.

Data Availability Statement

Data supporting the findings of this study are available upon reasonable request from the corresponding author.

Funding

This research received no external funding.

Acknowledgments

Declared none.

Conflicts of Interest

The authors declare no conflict of interest.

References

1. Bonchev, D. Chemical Graph Theory: Introduction and Fundamentals; Routledge: London, **1991**; https://doi.org/10.1201/9781315139104.
2. Trinajstic, N. Chemical Graph Theory, 2nd Edition; CRC Press: Boca Raton, **2018**; https://doi.org/10.1201/9781315139111.
3. van de Waterbeemd, H.; Carter, R.E.; Grassy, G.; Kubinyi, H.; Martin, Y.C.; Tute, M.S.; Willett, P. Glossary of terms used in computational drug design (IUPAC Recommendations 1997). *Pure Appl. Chem.* **1997**, *69*, 1137-1152, https://doi.org/10.1351/pac199769051137.
4. Randic, M. Characterization of molecular branching. *J. Am. Chem. Soc.* **1975**, *97*, 6609–6615, https://doi.org/10.1021/ja00856a001.
5. Randić, M. Novel molecular descriptor for structure—property studies. *Chem. Phys. Lett.* **1993**, *211*, 478–483, https://doi.org/10.1016/0009-2614(93)87094-J.
6. Shirakol, S.; Kalyanshetti, M.; Hosaman, S.M. QSPR analysis of certain distance based topological indices. *Appl. Math. Nonlinear Sci.* **2019**, *4*, 371-386, https://doi.org/10.2478/AMNS.2019.2.00032.
7. Wiener, H. Structural Determination of Paraffin Boiling Points. *J. Am. Chem. Soc.* **1947**, *69*, 17–20, https://doi.org/10.1021/ja01193a005.
8. Deutsch, E.; Klavžar, S. M-polynomial and Degree-based Topological Indices. *Iran. J. Math. Chem.* **2015**, *6*, 93-102, https://doi.org/10.22052/ijmc.2015.10106.
9. Mishra, R.K.; Sarkar, J.; Verma, K.; Chianella, I.; Goel, S.; Nezhad, H.Y. Borophene: A 2D wonder shaping the future of nanotechnology and materials science. *Nano Mater. Sci.* **2025**, *7*, 198-230, https://doi.org/10.1016/j.nanoms.2024.03.007.
10. Tatullo, M.; Zavan, B.; Genovese, F.; Codispoti, B.; Makeeva, I.; Rengo, S.; Fortunato, L.; Spagnuolo, G. Borophene Is a Promising 2D Allotropic Material for Biomedical Devices. *Appl. Sci.* **2019**, *9*, 3446, https://doi.org/10.3390/app9173446.
11. Wang, Z.-Q.; Lü, T.-Y.; Wang, H.-Q.; Feng, Y.P.; Zheng, J.-C. Review of borophene and its potential applications. *Front. Phys.* **2019**, *14*, 33403, https://doi.org/10.1007/s11467-019-0884-5.
12. Shao, W.; Tai, G.; Hou, C.; Wu, Z.; Wu, Z.; Liang, X. Borophene-Functionalized Magnetic Nanoparticles: Synthesis and Memory Device Application. *ACS Appl. Electron. Mater.* **2021**, *3*, 1133-1141, https://doi.org/10.1021/acsaelm.0c01004.
13. Munir, M.; Nazeer, W.; Nizami, A.R.; Rafique, S.; Kang, S.M. M-Polynomials and Topological Indices of Titania Nanotubes. *Symmetry* **2016**, *8*, 117, https://doi.org/10.3390/sym8110117.
14. Munir, M.; Nazeer, W.; Rafique, S.; Nizami, A.R.; Kang, S.M. Some Computational Aspects of Boron Triangular Nanotubes. *Symmetry* **2017**, *9*, 6, https://doi.org/10.3390/sym9010006.
15. Cheng-Peng, L.; Cheng, Z.; Mobeen, M.; Kalsoom, Y.; Jia-bao, L. M-polynomials and topological indices of linear chains of benzene, napthalene and anthracene. *Math. Biosci. Eng.* **2020**, *17*, 2384-2398, https://doi.org/10.3934/mbe.2020127.
16. Afzal, D.; Hussain, S.; Aldemir, M.S.; Farahani, M.R.; Afzal, F. New degree-based topological descriptors *via* m-polynomial of boron α-nanotube. *Eurasian Chem. Commun.* **2020**, *2*, 1117-1125.
17. Liu, J.B.; Younas, M.; Habib, M.; Yousaf, M.; Nazeer, W. M-Polynomials and Degree-Based Topological Indices of VC_5C_7[p,q] and HC_5C_7[p,q] Nanotubes. *IEEE Access* **2019**, *7*, 41125-41132, https://doi.org/10.1109/ACCESS.2019.2907667.

18. Julietraja, K.; Venugopal, P. Computation of Degree-Based Topological Descriptors Using M-Polynomial for Coronoid Systems. *Polycycl. Aromat. Compd.* **2022**, *42*, 1770–1793, https://doi.org/10.1080/10406638.2020.1804415.
19. Khan, A.R.; Ghani, M.U.; Ghaffar, A.; Asif, H.M.; Inc, M. Characterization of Temperature Indices of Silicates. *Silicon* **2023**, *15*, 6533-6539, https://doi.org/10.1007/s12633-023-02298-6.
20. Ismail, R.; Baby, A.; Xavier, D.A.; Varghese, E.S.; Ghani, M.U.; Nair, A.T.; Karamti, H. A novel perspective for M-polynomials to compute molecular descriptors of borophene nanosheet. *Sci. Rep.* **2023**, *13*, 12016, https://doi.org/10.1038/s41598-023-37637-5.
21. Nagesh, H.M. QSPR Analysis with Curvilinear Regression Modeling and Temperature-Based Topological Indices. *arXiv preprint arXiv:2404.08650* **2024**, https://doi.org/10.48550/arXiv.2404.08650.
22. Khan, A.R.; Ullah, Z.; Imran, M.; Malik, S.A.; Alamoudi, L.M.; Cancan, M. Molecular temperature descriptors as a novel approach for QSPR analysis of Borophene nanosheets. *PLOS ONE* **2024**, *19*, e0302157, https://doi.org/10.1371/journal.pone.0302157.
23. Sarhan, N.T.; Abdulkhaleq Ali, D.; Mohiaddin, G.H. M-Polynomial and Degree-Based Topological Indices forIterative Graphs. *Eur. J. Pure Appl. Math.* **2025**, *18*, 5711, https://doi.org/10.29020/nybg.ejpam.v18i1.5711.
24. Sajjad, W.; Reza Farahani, M.; Alaeiyan, M.; Hamid Hosseini, S.; Cancan, M. Computation of Eccentricity based topological properties of a Carbon Nanotube. *Arch. Sci.* **2025**, *75*, 17–30, https://doi.org/10.62227/as/75104.
25. Rilwan, N.M.; Bharathi, R.D. Exploring the degree based topological indices through M-polynomial and entropy measures of porous graphitic framework via logarithmic regression analysis. *Chem. Pap.* **2026**, *80*, 1491-1503, https://doi.org/10.1007/s11696-025-04465-y.
26. Venkatesan, A.; Binthiya, R.; Roopa, B.; Bala, A.J.K. Investigating the Use of M-Polynomial for Calculating Topological Indices in Carbazole Dendrimers. *Math. Stat.* **2025**, *13*, 181–193, https://doi.org/10.13189/ms.2025.130401.
27. Mehiri, E.-M. Explicit M-Polynomial and Degree-Based Topological Indices of Generalized Hanoi Graphs. *arXiv preprint arXiv:2511.12587* **2025**, https://doi.org/10.1016/j.dam.2026.03.006.
28. Mortazavi, B.; Rahaman, O.; Dianat, A.; Rabczuk, T. Mechanical responses of borophene sheets: a first-principles study. *Phys. Chem. Chem. Phys.* **2016**, *18*, 27405-27413, https://doi.org/10.1039/C6CP03828J.
29. Balakrishnan, R.; Ranganathan, K. A Textbook of Graph Theory; Springer: New York, NY, **2012**; https://doi.org/10.1007/978-1-4614-4529-6.
30. Bondy, A.; Murty, U.S.R. Graph Theory; Springer: London, **2008**.
31. Gutman, I.; Trinajstić, N. Graph theory and molecular orbitals. Total φ-electron energy of alternant hydrocarbons. *Chem. Phys. Lett.* **1972**, *17*, 535-538, https://doi.org/10.1016/0009-2614(72)85099-1.
32. Ilić, A.; Zhou, B. On reformulated Zagreb indices. *Discrete Appl. Math.* **2012**, *160*, 204–209, https://doi.org/10.1016/j.dam.2011.09.021.
33. Astaneh-Asl, A.; Fath-Tabar, G.H. Computing the First and Third Zagreb Polynomials of Cartesian Product of Graphs. *Iran. J. Math. Chem.* **2011**, *2*, 73–78, https://doi.org/10.22052/ijmc.2011.5177.
34. Jahanbani, A.; Shooshtary, H. Nano-Zagreb Index and Multiplicative Nano-Zagreb Index of Some Graph Operations. *Int. J. Comput. Sci. Appl. Math.* **2019**, *5*, 15–22.
35. Fansury, M.C.; Rinurwati. Sum Nano-Zagreb Index of Some Graph Operations. *J. Phys.: Conf. Ser.* **2020**, *1490*, 012040, https://doi.org/10.1088/1742-6596/1490/1/012040.
36. Shirdel, G.H.; Rezapour, H.; Sayadi, A.M. The Hyper-Zagreb Index of Graph Operations. *Iran. J. Math. Chem.* **2013**, *4*, 213–220, https://doi.org/10.22052/ijmc.2013.5294.
37. Vukičević, D.; Gašperov, M. Bond Additive Modeling 1. Adriatic Indices. *Croat. Chem. Acta* **2010**, *83*, 243-260.
38. Estrada, E.; Torres, L.; Rodríguez, L.; Gutman, I. An atom-bond connectivity index: Modelling the enthalpy of formation of alkanes. *Indian J. Chem.* **1998**, *37A*, 849-855.
39. Vukičević, D.; Furtula, B. Topological index based on the ratios of geometrical and arithmetical means of end-vertex degrees of edges. *J. Math. Chem.* **2009**, *46*, 1369–1376, https://doi.org/10.1007/s10910-009-9520-x.
40. Fajtlowicz, S. On conjectures of Graffiti. *Discrete Math.* **1988**, *72*, 113–118, https://doi.org/10.1016/0012-365X(88)90199-9.
41. Favaron, O.; Mahéo, M.; Saclé, J.-F. Some eigenvalue properties in graphs (conjectures of Graffiti — II). *Discrete Math.* **1993**, *111*, 197–220, https://doi.org/10.1016/0012-365X(93)90156-N.

42. Zhou, B.; Trinajstić, N. On general sum-connectivity index. *J. Math. Chem.* **2010**, *47*, 210–218, https://doi.org/10.1007/s10910-009-9542-4.
43. Kulli, V.R. On *K* Banhatti Indices of Graphs. *J. Comput. Math. Sci.* **2016**, *7*, 213–218.
44. Kulli, V.R. New *K*-Banhatti Topological Indices. *Int. J. Fuzzy Math. Arch.* **2017**, *12*, 29–37, https://doi.org/10.22457/ijfma.v12n1a4.

Publisher's Note & Disclaimer